

FRITL: A Hybrid Method for Causal Discovery in the Presence of Latent Confounders

Wei Chen

CHENWEIDELIGHT@GMAIL.COM

School of Computer Science, Guangdong University of Technology, Guangzhou, 510006, China

Kun Zhang*

KUNZ1@CMU.EDU

Department of Philosophy, Carnegie Mellon University, Pittsburgh, PA 15213, USA

Ruichu Cai*

CAIRUICHU@GMAIL.COM

*School of Computer Science, Guangdong University of Technology, Guangzhou, 510006, China
Pazhou Lab, Guangzhou, 510330, China*

Biwei Huang

BIWEIH@ANDREW.CMU.EDU

Department of Philosophy, Carnegie Mellon University, Pittsburgh, PA 15213, USA

Joseph Ramsey

JDRAMSEY@ANDREW.CMU.EDU

Department of Philosophy, Carnegie Mellon University, Pittsburgh, PA 15213, USA

Zhifeng Hao

ZFHAO@GDUT.EDU.CN

School of Mathematics and Big Data, Foshan University, Foshan, 528000, China

Clark Glymour

CG09@ANDREW.CMU.EDU

Department of Philosophy, Carnegie Mellon University, Pittsburgh, PA 15213, USA

Editor:

Abstract

We consider the problem of estimating a particular type of linear non-Gaussian model. Without resorting to the overcomplete Independent Component Analysis (ICA), we show that under some mild assumptions, the model is uniquely identified by a hybrid method. Our method leverages the advantages of constraint-based methods and independent noise-based methods to handle both confounded and unconfounded situations. The first step of our method uses the FCI procedure, which allows confounders and is able to produce asymptotically correct results. The results, unfortunately, usually determine very few unconfounded direct causal relations, because whenever it is possible to have a confounder, it will indicate it. The second step of our procedure finds the unconfounded causal edges between observed variables among only those adjacent pairs informed by the FCI results. By making use of the so-called Triad condition, the third step is able to find confounders and their causal relations with other variables. Afterward, we apply ICA on a notably smaller set of graphs to identify remaining causal relationships if needed. Extensive experiments on simulated data and real-world data validate the correctness and effectiveness of the proposed method.

Keywords: causal discovery, latent confounder, linear non-Gaussian acyclic model, independence noise condition, constraint-based method

©2021 Wei Chen, Kun Zhang, Ruichu Cai, Biwei Huang, Joseph Ramsey, Zhifeng Hao, and Clark Glymour.

License: CC-BY 4.0, see <https://creativecommons.org/licenses/by/4.0/>. Attribution requirements are provided at <http://jmlr.org/papers/v1/meila00a.html>.

1. Introduction

Causal discovery is crucial for understanding the actual mechanism underlying events in fields such as neuroscience Sanchez-Romero et al. (2019), biology Sachs et al. (2005) and social networks Cai et al. (2016). In such areas, the aim of the inquiry is to discover causal relations among variables that are measured only indirectly. Unmeasured variables and their influence on measured variables are unknown prior to the inquiry. Various methods for discovering the causal structure from observed samples have been proposed. However, most of them assume that the system of variables is causal sufficient, which means no pairs of variables have an unmeasured common cause (also called a latent confounder) Spirtes et al. (2001). Real applications typically violate this assumption. For example, some variables might not be measured because of limitations in data collection, and other variables may not even be considered in the data collection design. Without considering the presence of latent confounders, these algorithms return some false causal relations. Thus, developing a causal discovery method in the presence of latent confounders is an important research topic.

Methods for finding latent confounders and their relationships began early in the 20th century in factor analysis and its applications. In the case of continuous variables, linear relationships among variables are widely used as the data-generation assumption in searches for structural equation models (SEMs). Recently SEMs have begun to employ non-Gaussian additive (unmeasured) disturbances for each variable. The LvLiNGAM Hoyer et al. (2008) algorithm, which uses overcomplete Independent Components Analysis (ICA) Eriksson and Koivunen (2004) Lewicki and Sejnowski (2000), has been proposed to estimate the causal relations among measured variables in systems with linearly related variables. Given the number of latent confounders and appropriate data, it can in principle identify the measured variables sharing a common cause or causes, as well as the causal relations between measured variables, but it requires latent confounders to be mutually independent. This independence is impractical when the number of variables is large. The algorithm easily falls into local optima, which produces estimation errors aggravated by high-dimensional data. The ParceLiNGAM Tashiro et al. (2014) and PairwiseLvLiNGAM Entner and Hoyer (2010) methods have been proposed for the same model class, but these methods fail to identify the causal structure given in Fig. 1. Existing independence noise-based methods have a high computational load and do not fully identify the causal structure.

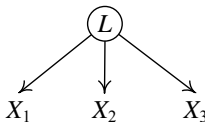


Figure 1: An example of a causal graph, where X_1 , X_2 and X_3 are observed variables, and L is a latent confounder.

Constraint-based methods such as the Fast Causal Inference (FCI) algorithm Spirtes et al. (2001) is another type of methods for recovering causal structures. Although the results of the FCI algorithm are statistically consistent but provide limited information. For example, even when no confounders exist, FCI usually provides too few directed, unconfounded causal relationships; on the other hand, for a small number of variable pairs, hidden variables usually can not be found. As a specific example, consider the data generated according to the Directed Acyclic Graph (DAG) shown in Figure 2(a). The FCI output, called Partial Ancestral Graph (PAG), is given as Figure 2(b). The adjacency and arrowheads in Figure 2(b) are mostly correct, but some undetermined tails of edges remain.

From these observations, we propose a hybrid method assuming linearity and non-Gaussianity, to take advantages of both constraint-based methods and independent noise-based methods to handle both confounded and unconfounded situations. However, designing such a solution is a non-trivial task due to the two specific challenges raised by the high dimensionality of the measured variables and the latent confounders. One is how to efficiently decompose a large global graph into local small structures without introducing new latent confounders. The second is how to recover local structures accurately in the presence of latent confounders. To address these challenges, we first employ FCI to remove some independent causal relationships. This output will not be complete, in the sense that it contains many undetermined causal edges when latent confounders might not exist. We further refine this output to examine unconfounded causal edges and locate the latent confounders by applying an independent noise-based method among only those adjacent pairs informed by the FCI result. The Triad condition Cai et al. (2019) identifies some shared latent confounders and the causal relations between measured variables. If some causal directions are still undetermined, we apply overcomplete ICA locally to refine the causal structure.

We summarize our contributions as follows:

- 1) We propose a hybrid framework to reconstruct the entire causal structure from measured data, handling both confounded and unconfounded situations.
- 2) We show the completeness result of our proposed method, demonstrating the correctness of our method on the theoretical side;
- 3) We verify the correctness and effectiveness of our method on simulated and real-world data, showing results to be mostly consistent with the background knowledge.

2. Graphical Models

We employ two types of graphical representations of causal relations: Directed Acyclic Graphs (DAGs) and Partial Ancestral Graphs (PAGs).

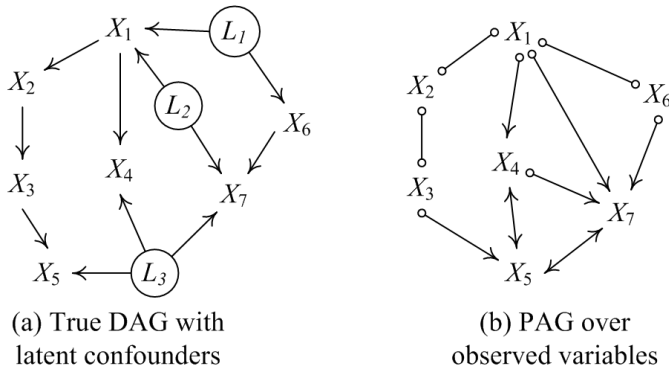


Figure 2: An example for graphs of observed variables X_1, X_2, \dots, X_7 and latent confounders L_1, L_2 and L_3 : (a) the original directed acyclic graph (DAG), and (b) the corresponding PAG produced by FCI.

2.1 DAG Description

A DAG can be used to represent both causal and independence relationships. A DAG contains a set of vertices and a set of directed edges (\rightarrow), where each vertex represents one random variable. $X_i \rightarrow X_j$ means that X_i is a “direct” cause (or parent) of X_j , that is, X_j is a direct effect (or child) of X_i . Figure 2(a) shows an example of a DAG \mathcal{G} . In Figure 2(a), X_1 is a parent of X_2 , or X_2 is a child of X_1 , due to the edge $X_1 \rightarrow X_2$. Two vertices (X_i, X_j) are adjacent if there is a directed edge $X_i \rightarrow X_j$ or $X_j \rightarrow X_i$. A directed path from X_i to X_j is a sequence of vertices beginning with X_i and ending with X_j such that each vertex in the sequence is a child of its predecessor in the sequence. Any sequence of vertices in which each vertex is adjacent to its predecessor is an undirected path. A vertex, in a path X_i is a collider if X_i is a child of both its predecessor and its successor in the path.

d-separation Pearl (1988). Let \mathbf{X} be a set of variables in DAG \mathcal{G} that does not have either of X_i and X_j as members. X_i and X_j are d-separated given \mathbf{X} if and only if there exists no undirected path U between X_i and X_j , such that both of the following conditions hold:

- (i) every collider on U has a descendent (or itself) in \mathbf{X} ;
- (ii) no variable on U that is not a collider is in \mathbf{X} .

Two variables that are not d-separated by \mathbf{X} are said to be d-connected given \mathbf{X} .

2.2 PAG Description

A PAG contains four different types of edges between two variables: directed edge (\rightarrow), bidirected edge (\leftrightarrow), partially directed edge ($\circ \rightarrow$), and nondirected edge ($\circ - \circ$). A directed

edge $X_i \rightarrow X_j$ means that X_i is a cause of X_j . A bidirected edge $X_i \leftrightarrow X_j$ indicates that there is a latent confounder that is a common cause of X_i and X_j . A partially directed edge $X_i \circ \rightarrow X_j$ indicates that either X_i is a cause of X_j , or there is an unmeasured variable influencing X_i and X_j , or both. A nondirected edge $X_i \circ - \circ X_j$ means exactly one of the following holds: (a) X_i is a cause of X_j ; (b) X_j is a cause of X_i ; (c) there is an unmeasured variable influencing X_i and X_j ; (d) both a and c; or (e) both b and c. In a PAG, the end marks of some edges may be undetermined, i.e., the undetermined edge is an edge other than the directed edge.

Figure 2(b) shows a PAG representing the set of all DAGs that imply the same conditional independence relations *among the measured variables* as does the DAG \mathcal{G} (Figure 2(a)). For example, the bidirected edge between X_4 and X_5 means that there is a latent confounder influencing X_4 and X_5 . The non-directed edge between X_1 and X_2 shows a class of causal relation between X_1 and X_2 , that is, this edge might be: $X_1 \rightarrow X_2$, $X_1 \leftarrow X_2$, $X_1 \leftrightarrow X_2$.

A PAG can be estimated by the FCI algorithm Spirtes et al. (2001) or one of its variants such as RFCI Colombo et al. (2012), FCI⁺ Claassen et al. (2013), FCI-stable Colombo and Maathuis (2014), Conservative FCI (CFCI) Ramsey et al. (2006) or Greedy FCI (GFCI) Ogarrio et al. (2016).

3. Problem Definition

To help with the definition of the scope of our solution, we assume that all samples are infinite, independent distributed, following the same joint probability distribution P . Further, we make some or all of the following assumptions according to context.

A1. Causal Markov Assumption. Two variables X_i and X_j are independent given a subset \mathbf{S} of variables not containing X_i and X_j , if X_i and X_j are d-separated given \mathbf{S} .

A2. Causal Faithfulness Assumption. Let $\mathbf{S} \cap \{X_i, X_j\} = \emptyset$. If X_i and X_j are independent conditional on \mathbf{S} in P , then X_i is d-separated from X_j conditional on \mathbf{S} in \mathcal{G} .

We assume the target to be discovered is a DAG, represented as a linear non-Gaussian model with latent confounders (named as LvLiNGAM), as defined by Hoyer et al. Hoyer et al. (2008), in which each measured variable X_i in \mathbf{X} , $i = 1, 2, \dots, n$, is generated from its parents including measured variables and latent confounders \mathbf{L} with an additive noise term. The matrix form of LvLiNGAM then can be formalized as

$$\mathbf{X} = \mathbf{B}\mathbf{X} + \Lambda\mathbf{L} + \mathbf{E}, \tag{1}$$

where \mathbf{B} is the matrix of causal strengths among measured variables, Λ is the matrix of causal influences of the latent confounders \mathbf{L} on measured variables, and the noise terms, as components of \mathbf{E} , are mutually independent and non-Gaussian. According to lvLiNGAM by Hoyer et al. Hoyer et al. (2008), we know that \mathbf{B} can be permuted to be a lower

triangular matrix, and Equation 1 can be changed to

$$\begin{aligned} \mathbf{X} &= \mathbf{B}\mathbf{X} + \Lambda\mathbf{L} + \mathbf{E}, \\ \Rightarrow \mathbf{X} &= (\mathbf{I} - \mathbf{B})^{-1}\Lambda\mathbf{L} + (\mathbf{I} - \mathbf{B})^{-1}\mathbf{E}, \\ \Rightarrow \mathbf{X} &= [(\mathbf{I} - \mathbf{B})^{-1}\Lambda \mid \mathbf{I}] \cdot \begin{bmatrix} \mathbf{L} \\ \mathbf{E} \end{bmatrix} = \mathbf{A} \cdot \begin{bmatrix} \mathbf{L} \\ \mathbf{E} \end{bmatrix}, \end{aligned} \tag{2}$$

where $\mathbf{A} := [(\mathbf{I} - \mathbf{B})^{-1}\Lambda \mid \mathbf{I}]$ and \mathbf{I} denotes the identity matrix.

Based on Equation 1, we make the following further assumptions:

A3. Linear Acyclic Non-Gaussianity Assumption. The causal graph over all variables, including the latent variables, is a directed acyclic graph (DAG), which represents the model in which the causal relations among any variables are linear and all noise terms are non-Gaussian and mutually independent.

A4. One Latent Confounder Assumption. All latent confounders are independent of each other, and each pair of observed variables is directly influenced by at most one latent confounder.

Based on the above assumptions, we define our problem as follows.

Definition 1. (Problem Definition) *Given the observational data generated by causal model as Equation 1, reconstruct the causal graph over measured variables and latent confounders.*

4. A Hybrid Method for Causal Discovery in the Presence of Latent Confounders

In this section, we describe our approach in detail, and explaining how it recover the true graph shown in Figure 3(a) that represents causal model (1). The proposed framework is given in Figure 3.

The idea is as follows. After running the FCI algorithm to obtain a PAG, we further try to orient edges by regression and subsequent independence testing, extrapolating directions by the well-known Meek rules. From regression residuals, we further determine local causal structures for pairs of variables that are adjacent with an undetermined edge in the PAG. We then introduce a constraint condition for triples of variables to detect and combine some latent confounders. Finally, under the further assumption that the latent confounders are independent, we use overcomplete ICA to determine the remaining edges when needed. The pseudo-code of this framework (named FRITL) is described in Algorithm 1. The use of these four steps can be selected according to the purpose.

4.1 Stage I: Constructing PAG Using FCI

We begin by supposing that the data generated by causal model (1) satisfies assumptions **A1-A2**. The FCI algorithm outputs a PAG, which represents estimated features of the true causal DAG according to the following theorem Spirtes et al. (2001) and lemma.

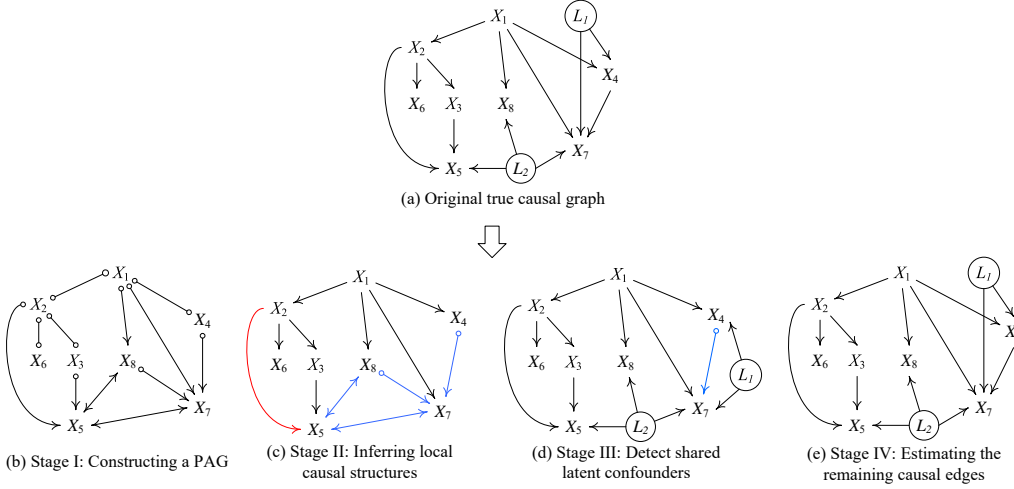


Figure 3: The proposed framework. In these graphs, X_1, X_2, \dots, X_8 represent the measured variables and L_1 and L_2 represent the latent confounders. The red line in (c) means the edge $X_2 \rightarrow X_5$ can be updated by FCI orientation rule \mathcal{R}_8 . Blue lines in (c) and (d) indicate the edges for which end marks are not determined.

Algorithm 1 FRITL Algorithm

Input: Data \mathcal{D} , threshold for independence test α

Output: Causal graph \mathcal{G}_{out} over measured variables and latent confounders

Stage I: Construct a PAG \mathcal{G}_1 by running the FCI algorithm on \mathcal{D} ;

Stage II: Infer local causal structures by using an independence noise condition for undetermined adjacent pairs of variables in \mathcal{G}_1 ; update \mathcal{G}_1 to \mathcal{G}_2 ;

Stage III: Detect shared latent confounders by using Triad conditions and update \mathcal{G}_2 to \mathcal{G}_3 ;

Stage IV: Estimate remaining undetermined local causal structures in \mathcal{G}_3 using over-complete ICA. Update \mathcal{G}_3 to \mathcal{G}_{out} .

Theorem 1. Given the assumptions **A1-A2**, the FCI algorithm outputs a PAG that represents a class of graphs including the true causal DAG.

Lemma 1. Given the assumptions **A1-A2**, if FCI converges to a PAG with a directed edge between X_i and X_j , then there is a directed edge between X_i and X_j in the true DAG.

We first apply FCI on the data to obtain a PAG. For example, using the graph representing a lvLiNGAM model in Figure 3(a), the FCI algorithm outputs the PAG shown in Figure 3(b).

4.2 Stage II: Inferring Local Structures Using Independence Noise Condition

After running stage I, we obtain the PAG (given in Figure 3(b)) that is (asymptotically) correct information of the causal structure but usually provides few direct influences. Although we can apply overcomplete ICA to estimate the true causal graph, the result may suffer from local optima, especially if the number of measured variables is larger than four. In contrast, the “divide-and-conquer” provides more causal information about the undetermined edges in the graph and only requires performing overcomplete ICA on a small number of variables to estimate the local causal structures. This second stage produces correct, informative causal discovery result with relatively low computational complexity. We note that in the linear non-Gaussian case, unconfounded causal relations can always be determined by regression and independence testing Shimizu et al. (2011). Inspired by this, we consider generalizing regression and independence test from global causal structure to local causal structure, even when there are latent confounders.

4.2.1 IDENTIFICATION OF CAUSAL DIRECTION BETWEEN UNCONFOUNDED PAIRS OF VARIABLES

We first provide a lemma to identify the causal direction of variables that are not influenced by confounders. Let \mathcal{G} denote the PAG obtained by FCI. From the definition of a PAG, variables connected to the measured variable X_i through a directed, nondirected, or partially directed edge are the potential parents of X_i . For example, X_j is a potential parent of X_i if $X_j \rightarrow X_i$, $X_j \circ\text{-}\circ X_i$, or $X_j \circ\text{-}\rightarrow X_i$. Let $X_{\text{par}(i)}$ denote the potential parents of X_i in \mathcal{G} .

If there are no latent or observed confounders of X_i and any of $X_{\text{par}(i)}$, we can generalize Lemma 1 proposed by Shimizu et al. Shimizu et al. (2011) to determine local causal structures. We first introduce the Darmois-Skitovitch Theorem Darmois (1953)Skitovitch (1953), which determines whether each potential parent is an actual parent of X_i .

Theorem 2. (Darmois-Skitovitch Theorem). *Define two random variables X_1 and X_2 , as linear combinations of independent random variables $S_i, i = 1, \dots, n$:*

$$X_1 = \sum_{i=1}^n \alpha_i S_i, X_2 = \sum_{i=1}^n \beta_i S_i. \quad (3)$$

If X_1 and X_2 are statistically independent, then all variables S_j for which $\alpha_j \beta_j \neq 0$ are Gaussian.

In other words, if random variables $S_i, i = 1, \dots, n$ are independent and for some $\alpha_1, \alpha_2, \dots, \alpha_n$ and $\beta_1, \beta_2, \dots, \beta_n$, X_1 is independent of X_2 , then for any S_j that is non-Gaussian, at most one of α_j and β_j can be nonzero.

Lemma 2. *Suppose that the data over variables \mathbf{X} are generated by (1) and that assumptions **A1-A3** hold. Assume there is no latent or observed confounder relative to X_i and*

X_j in the underlying true causal graph over all given variables, where X_j is one of the potential parents of X_i in the FCI output. Let $R_{i,j}$ be the residual of the regression of X_j on X_i . Then in the limit of infinite data, X_i is an unconfounded ancestor of X_j if and only if $X_i \perp\!\!\!\perp R_{j,i}$ and $X_j \not\perp\!\!\!\perp R_{i,j}$.

Proof. Without loss of generality, all these data are normalized to have zero mean and unit variance.

1. Assume that X_i is an ancestor of X_j and that X_i is an exogenous variable, which means that there are no parent or latent confounders for X_i and X_j . X_i and X_j are generated by (1). This leads to

$$\begin{aligned} X_i &= E_i, \\ X_j &= b_{j,i}X_i + E_j^{(-i)}, \end{aligned} \tag{4}$$

where $E_j^{(-i)} = \sum_{k \in \mathbf{par}(j), k \neq i} b_{j,k}X_k + E_j$ and X_i are independent.

(1) The residual of regressing X_j on X_i will be

$$\begin{aligned} R_{j,i} &= X_j - \frac{\text{Cov}(X_j, X_i)}{\text{Var}(X_i)} \cdot X_i \\ &= (b_{j,i}X_i + E_j^{(-i)}) - b_{j,i}X_i \\ &= E_j^{(-i)}. \end{aligned} \tag{5}$$

Thus, the residual $R_{j,i}$ is independent of X_i because $E_j^{(-i)}$ is independent of X_i .

(2) If instead we regress X_i on X_j , the residual will be

$$\begin{aligned} R_{i,j} &= X_i - \frac{\text{Cov}(X_i, X_j)}{\text{Var}(X_j)} \cdot X_j \\ &= E_i - \frac{\text{Cov}(X_i, X_j)}{\text{Var}(X_j)} \cdot (b_{j,i}X_i + E_j^{(-i)}) \\ &= \left(1 - \frac{\text{Cov}(X_i, X_j)}{\text{Var}(X_j)}\right) \cdot E_i - \frac{b_{j,i}\text{Cov}(X_i, X_j)}{\text{Var}(X_j)} \cdot \sum_{k \in \mathbf{par}(j), k \neq i} b_{j,k}X_k \\ &\quad - \frac{b_{j,i}\text{Cov}(X_i, X_j)}{\text{Var}(X_j)} E_j. \end{aligned} \tag{6}$$

Each parent of X_j is a linear mixture of error terms including E_j , where all the error terms are mutually independent and non-Gaussian according to assumption **A3**. Thus, the residual $R_{i,j}$ is a mixture of E_i , E_j , and $X_k (k \in \mathbf{par}(j), k \neq i)$, where each $X_k (k \in \mathbf{par}(j), k \neq i)$ is non-Gaussian. From Equations (4) and (6), the coefficient of E_j is non-zero, which implies that X_j is dependent of $R_{i,j}$ according to Theorem 2. Thus, if X_i is an ancestor of X_j , then X_i is dependent of $R_{j,i}$ and X_j is dependent of $R_{i,j}$.

2. Assume that X_i and X_j have at least one common ancestor. Let $X_{\mathbf{Pa}_i}$ denote all parents of X_i , and X_k be an actual parent of X_i . Then we have

$$X_i = \sum_{k \in \mathbf{Pa}_i} b_{i,k} X_k + E_i. \quad (7)$$

If we regress X_j on X_i , the residual $R_{j,i}$ will be

$$\begin{aligned} R_{j,i} &= X_j - \frac{Cov(X_i, X_j)}{Var(X_i)} \cdot X_i \\ &= X_j - \frac{Cov(X_i, X_j)}{Var(X_i)} \cdot \left(\sum_{k \in \mathbf{Pa}_i} b_{i,k} X_k + E_i \right) \\ &= \left(1 - \frac{b_{i,j} Cov(X_i, X_j)}{Var(X_i)} \right) \cdot X_j - \frac{Cov(X_i, X_j)}{Var(X_i)} \cdot \sum_{k \in \mathbf{Pa}_i, k \neq j} b_{i,k} X_k \\ &\quad - \frac{Cov(X_i, X_j)}{Var(X_i)} \cdot E_i. \end{aligned} \quad (8)$$

Each parent of X_i is a linear mixture of error terms other than E_i , with all the error terms mutually independent and non-Gaussian according to assumption **A3**. Thus, the residual $R_{j,i}$ can be written as a linear mixture of error terms including E_i . We can see that the coefficient of E_i in Equations (7) and (8) is nonzero due to $Cov(X_i, X_j) \neq 0$, which implies that X_i is dependent of $R_{j,i}$ according to Theorem 2. \square

Lemma 2 provides a principle to determine the causal direction between a pair of measured variables. If there is no latent or observed confounder for X_i and other variables, we can find the ancestors and children of X_i . In detail, for each variable X_j in $X_{\mathbf{par}(i)}$, we regress X_i on X_j and test whether the residual is independent of X_j . At the same time, we regress X_j on X_i and test the independence between the residual and X_i . Then according to Lemma 2, we can determine whether X_j is an ancestor or child of X_i , or whether there is a confounder for them.

If we have determined some parents or children for measured variable X_i , we can remove the common cause for two measured variables that are adjacent with the determined causal relationship by regression Shimizu et al. (2011), and then perform the step as above. This can determine most of the undetermined causal relations that are not influenced by confounders.

4.2.2 IDENTIFICATION OF CAUSAL DIRECTION BETWEEN VARIABLES NOT DIRECTLY INFLUENCED BY THE SAME CONFOUNDER

After identifying the unconfounded ancestor, some cases where the causal structure between the measured variables cannot be identified because of the indirect latent confounders. They contain two cases:

1. The parent and children of the measured variable X_i are directly influenced by the same latent confounder L_j , while X_i is not adjacent to (or equivalently, not directly influenced by) L_j ;
2. Two or more parents of the measured variable X_i are influenced by the same latent confounder L_j , while X_i is not adjacent to L_j .

Case 1: For the first case, and using Figure 4(a) as an example, X_1 and X_3 are directly influenced by the hidden common cause L_1 , but X_2 is not. The PAG obtained by Stage I is shown in 4(b). Then for any of the three pairs of the three variables X_1 , X_2 , and X_3 , regression is performed, and the independence of the residuals and the predictor variable is tested. But we can only determine $X_1 \rightarrow X_2$, and cannot identify $X_2 - X_3$. If we can remove the indirect cause of X_2 , then $X_2 - X_3$ can be determined. After determining that $X_1 \rightarrow X_2$, we regress X_2 on X_1 and replace X_2 with its corresponding residual $R_{2,1}$. We can find that if the causal relationship between $R_{2,1}$ and X_3 also satisfies model (1), we can use Lemma 2 to determine $X_2 \rightarrow X_3$. Next, we generalize Lemma 2 proposed by Shimizu et al. Shimizu et al. (2011) to the latent confounder case and call it Lemma 3.

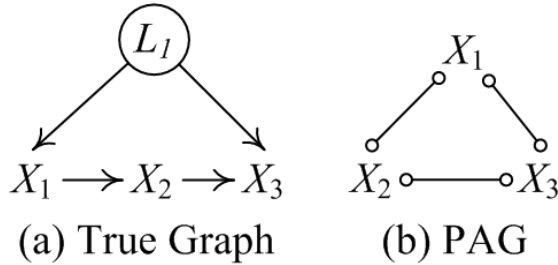


Figure 4: An example that cannot be identified by Lemma 2: (a) a true causal graph; (b) the PAG estimated by Stage I using the data generated according to (a). In these graphs, X_1, X_2 , and X_3 represent the measured variables while L_1 represents a latent confounder.

Lemma 3. *Assume that the data over measured variables \mathbf{X} follows Model (1). Let $\mathbf{X}_{\mathbf{Pa}_i}$ denote a set of all found parents of X_i ($X_i \in \mathbf{X}$) and \mathbf{R} be the result of replacing each X_i with its residual from regressing on $\mathbf{X}_{\mathbf{Pa}_i}$. Then, an analog of Model (1) holds as follows: $\mathbf{R} = \mathbf{B}_R \mathbf{R} + \Lambda \mathbf{L} + \mathbf{E}_R$, where \mathbf{B}_R is a matrix of causal strengths among the residuals that corresponds to the measured variables, Λ is a matrix of causal influences of the latent confounders \mathbf{L} on measured variables, and the noise terms in \mathbf{E}_R are mutually independent and non-Gaussian.*

Proof. Without loss of generality, we assume that \mathbf{B} in Equation 2 can be permuted to a strictly lower triangular matrix. Therefore, \mathbf{A} of Equation 2 is also a lower triangular

matrix with diagonal entries. Since $X_{\mathbf{Pa}_i}$ is the parent of X_i for each X_i , $\mathbf{A}_{i,\mathbf{Pa}_i}$ is equal to the regression coefficient obtained by linear regression of X_i on $X_{\mathbf{Pa}_i}$. Therefore, through linear regression, the causal effect of $X_{\mathbf{Pa}_i}$ on X_i is removed from X_i , that is, each $A_{i,j}$ in $\mathbf{A}_{i,\mathbf{Pa}_i}$ is 0, and $X_{\mathbf{Pa}_i}$ does not influence the residual $\mathbf{R}_{i,\mathbf{Pa}_i}$. Therefore, for \mathbf{R} , its corresponding $\tilde{\mathbf{A}}$ is still a strictly lower triangular matrix, (i.e., $\tilde{\mathbf{B}}$ is also a strictly lower triangular matrix). Therefore, $\mathbf{R} = \mathbf{B}_R \mathbf{R} + \Lambda \mathbf{L} + \mathbf{E}_R$ holds. \square

Thus, for each variable X_i , after removing the effect of all determined parents of X_i by regressions and independence tests we can find the parents and children of X_i . The details of the procedure are as follows.

First, for each pair of measured variables X_i and X_j , we perform a linear regression of X_i on X_j , and test whether the corresponding residual $R_{i,j}$ is independent of X_j . If it is, we orient $X_j \rightarrow X_i$. Otherwise, we test whether the reverse causal direction is accepted. If neither of them is accepted, there may be at least one latent confounder or a common ancestor influencing them. After refining some edges, we remove the effects of parents by regressing the variable on its determined parents and using the corresponding residuals to replace the variables. This is because if X_i and X_j are unconfounded, then after we remove the information in X_i and X_j that can be explained by their common ancestors, the residuals in X_i and X_j are unconfounded and they admit the same causal direction as that between X_i and X_j . Then, we iterate the first step for the variables with an undetermined edge between them to determine more edges, until no independence between a potential parent of variable and the corresponding residual is accepted.

Case 2: We then consider the second case for X_i and its parents X_j and X_k ; we still cannot determine the causal relationship between X_i and X_j or between X_i and X_k . That is to say, X_j and X_k are mediating variables for the path from L and X_i so that L is a common cause of X_i and X_j , and of X_i and X_k . Using X_k to “block” this path will remove the influence from L to X_i . This inspired us to apply regressions to address the problem, with the following theorem confirming its correctness.

Lemma 4. *Suppose that the data over variables \mathbf{X} were generated by Equation 1 and assumptions **A1**–**A3** hold. Let $X_{\mathbf{par}(i)}$ denote a set of measured variables that are potential parents of X_i and $X_{\mathbf{S}_i} \subset X_{\mathbf{par}(i)}$. Let R_{i,\mathbf{S}_i} be the residual of regressing X_i on $X_{\mathbf{S}_i}$. In the limit of infinite data, X_j is an unconfounded parent of X_i , if and only if there exist a subset $X_{\mathbf{S}_i}$, defined above such that X_j is independent of R_{i,\mathbf{S}_i} .*

Proof. Note that $X_{\mathbf{par}(i)}$ denote all potential parents of X_i and $X_{\mathbf{S}_i}$ be a subset of $X_{\mathbf{par}(i)}$. If variable X_j is in $X_{\mathbf{par}(i)}$, then X_j might be a (confounded) parent or child of X_i , or there is a latent confounder between X_i and X_j without directed edge.

1. Consider that X_j is a parent of X_i and there is no latent confounder between X_i and X_j . First, we can rewrite Equation 1 as

$$\begin{aligned} \mathbf{X} = \begin{pmatrix} X_{\mathbf{S}_i} \\ X_i \end{pmatrix} &= (\mathbf{I} - \mathbf{B})^{-1}(\Lambda \mathbf{L} + \mathbf{E}) = \mathbf{C}(\Lambda \mathbf{L} + \mathbf{E}) \\ &= \begin{bmatrix} \mathbf{C}_{\mathbf{S}_i} & \mathbf{C}_{\mathbf{S}_i, i}^T \\ \mathbf{C}_{i, \mathbf{S}_i} & 1 \end{bmatrix} \begin{bmatrix} \Lambda_{X_{\mathbf{S}_i}} \mathbf{L} + E_{\mathbf{S}_i} \\ \Lambda_i \mathbf{L} + E_i \end{bmatrix}, \end{aligned}$$

where $\mathbf{C} = (\mathbf{I} - \mathbf{B})^{-1}$. The inverse of \mathbf{C} can be written as

$$\mathbf{C}^{-1} = \begin{bmatrix} \mathbf{D}^{-1} & -\mathbf{C}_{\mathbf{S}_i, i}^T \mathbf{D}^{-1} \\ -\mathbf{D}^{-1} \mathbf{C}_{i, \mathbf{S}_i} & (1 - \mathbf{C}_{\mathbf{S}_i, i}^T \mathbf{C}_{\mathbf{S}_i}^{-1} \mathbf{C}_{i, \mathbf{S}_i})^{-1} \end{bmatrix}, \quad (9)$$

where $\mathbf{D} = \mathbf{C}_{\mathbf{S}_i} - \mathbf{C}_{\mathbf{S}_i, i}^T \mathbf{C}_{i, \mathbf{S}_i}$. Thus, $1 - \mathbf{C}_{\mathbf{S}_i, i}^T \mathbf{C}_{\mathbf{S}_i}^{-1} \mathbf{C}_{i, \mathbf{S}_i} = 1$.

Then, regressing X_i on $X_{\mathbf{S}_i}$, we have

$$\begin{aligned} R_{i, \mathbf{S}_i} &= X_i - \frac{\mathbb{E}[X_i, X_{\mathbf{S}_i}]}{\mathbb{E}[X_{\mathbf{S}_i}^2]} X_{\mathbf{S}_i} \\ &= \mathbf{C}_{i, \mathbf{S}_i} (\Lambda_{X_{\mathbf{S}_i}} \mathbf{L} + \mathbf{E}_{\mathbf{S}_i}) + (\Lambda_i \mathbf{L} + E_i) \\ &\quad - \alpha_{i, \mathbf{S}_i} (\mathbf{C}_{\mathbf{S}_i} (\Lambda_{X_{\mathbf{S}_i}} \mathbf{L} + \mathbf{E}_{\mathbf{S}_i}) + \mathbf{C}_{\mathbf{S}_i, i}^T (\Lambda_i \mathbf{L} + E_i)) \\ &= \{\mathbf{C}_{i, \mathbf{S}_i} \Lambda_{X_{\mathbf{S}_i}} + \Lambda_i - \alpha_{i, \mathbf{S}_i} (\mathbf{C}_{\mathbf{S}_i, i} \Lambda_{X_{\mathbf{S}_i}} + \mathbf{C}_{\mathbf{S}_i, i}^T \Lambda_i)\} \mathbf{L} \\ &\quad + (\mathbf{C}_{i, \mathbf{S}_i} - \alpha_{i, \mathbf{S}_i} \mathbf{C}_{\mathbf{S}_i}) \mathbf{E}_{\mathbf{S}_i} + (1 - \alpha_{i, \mathbf{S}_i} \mathbf{C}_{\mathbf{S}_i, i}^T) E_i, \end{aligned}$$

where $\alpha_{i, \mathbf{S}_i} = \frac{\mathbb{E}[X_i, X_{\mathbf{S}_i}]}{\mathbb{E}[X_{\mathbf{S}_i}^2]}$.

Thus, the residual R_{i, \mathbf{S}_i} will be a linear mixture of latent confounders, the noise terms of X_i and all variables in $X_{\mathbf{S}_i}$. If the linear contributions of all variables in $X_{\mathbf{S}_i} \setminus X_j$ to the influence of X_j on X_i have been partialled out, that is, $\mathbf{C}_{i, \mathbf{S}_i} - \alpha_{i, \mathbf{S}_i} \mathbf{C}_{\mathbf{S}_i} = \mathbf{0}^T$, then we can obtain

$$\begin{aligned} R_{i, \mathbf{S}_i} &= \Lambda_i (1 - \alpha_{i, \mathbf{S}_i} \mathbf{C}_{\mathbf{S}_i, i}^T) \mathbf{L} + (1 - \alpha_{i, \mathbf{S}_i} \mathbf{C}_{\mathbf{S}_i, i}^T) E_i \\ &= \Lambda_i \mathbf{L} + E_i. \end{aligned} \quad (10)$$

Because there is no latent confounder between X_i and X_j , the coefficient of \mathbf{L} on X_j is zero. Thus, from Equation 10, R_{i, \mathbf{S}_i} is independent of X_j due to Theorem 2.

2. Consider that X_j is a confounded parent or confounded child of X_i , or that there is a latent confounder between them without directed edge. The effect of the latent confounder may not vanish by multiple regression on any measured variables. So the residual of regressing X_i on $X_{\mathbf{S}_i}$ ($X_j \in X_{\mathbf{S}_i}$) is dependent of X_j .

3. Consider that X_j is a child of X_i and there is no latent confounder between X_i and X_j . If we regress X_i on every $X_{\mathbf{S}_i}$ which contains X_j , the residual R_{i, \mathbf{S}_i} will be a linear mixture of the noise term of X_i and others. According to the Equation 1, R_{i, \mathbf{S}_i} is a linear mixture of the noise term of X_i , X_j and others. Thus, X_j is dependent of R_{i, \mathbf{S}_i} . \square

Lemma 4 inspires a method of identifying the local structure of measured variables for the second case by analyzing the PAG. According to Lemma 4, we start by performing a multiple regression of undetermined variable X_i on every subset of its potential parents to test whether there exist *two* variables X_j and X_k such that the corresponding residual is independent of these two variables. If the independence holds for variable X_j and the residual, then X_j is a parent of X_i . Similarly, if undetermined edges remain, we perform a multiple regression on the subset of the potential parents containing *three* variables and then *four* variables, and so on, to find variables in the subset of potential parents that are unconfounded parents (according to independence tests) until no subset such that the residual is independent of the predictor(s) can be found.

Using these methods, we find local causal structures over measured variables that are adjacent to an undetermined edge in \mathcal{G} . In this stage, when an edge is reoriented, we apply FCI orientation rules Zhang (2008) to orient other undetermined edges and update the corresponding potential parent sets. Using these orientation rules saves a number of regressions and independence tests.

As an example, using the causal graph from Figure 3(b), we obtain the output by (multiple) regressions and independence tests. By applying the FCI orientation rule $\mathcal{R}8$ Zhang (2008), we reorient the edge between X_2 and X_5 according to assumption **A3**. The final graph produced by this stage is shown in Figure 3(c).

According to the stage II process, the following theorem summarizes identifiability.

Theorem 3. *Suppose that the data over variables \mathbf{X} was generated by model (1) and assumptions **A1** – **A3** hold. Let \mathcal{G}_1 denote the output of stage I. The pairs of variables with an undirected edge in between in \mathcal{G}_1 that are not actually directly influenced by the same latent confounder are identified by stage II of FRITL.*

Proof. Under the assumptions of the theorem, stage I removes most of the independent causal edges, which provides stage II with (conditional) independence information. With the help of Lemmas 2 and 3, we can determine the direction of the causal relationship between variables that are not directly influenced by the same latent confounder. Lemma 4 provides the identifiability conditions of the causal structure between observed variables that are not influenced by the same latent confounder. \square

As a consequence, what remains to be identified is the causal structure between variables directly influenced by the same latent confounders.

4.3 Stage III: Detecting Shared Latent Confounders Using the Triad Condition

The procedure so far determines whether latent confounders exist in many cases, but some graphs corresponding to the PAG shown in Figure 5 remain undistinguishable. Stage II only considers two variables each time. Thus, there are no details about the causal relationship

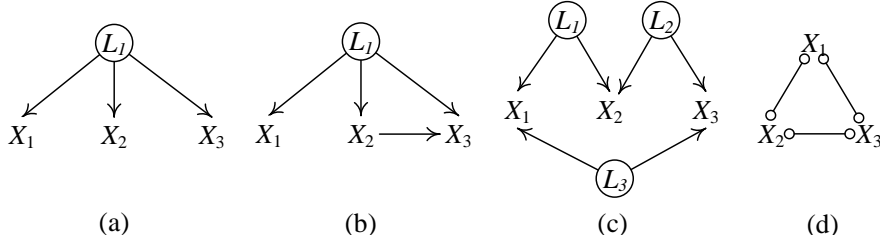


Figure 5: The three causal graphs in (a), (b), and (c) all correspond to the completed nondirected PAG obtained by FCI shown in (d). They cannot be distinguished by stage II of our method.

(e.g., whether there is a direct causal relation and which way the causal influence goes) between two variables that are directly influenced by a same latent confounder, because these two variables both contain the information of the latent confounder. Suppose that assumptions **A3** hold. Interestingly, if we consider another measured variable at the same time, we can treat this third variable as a “conditional variable” or an “instrumental variable” and use it to help remove the indirect causal relationship (due to the existence of latent confounders) through the path containing latent confounders. The Triad condition Cai et al. (2019), which the proposed procedure makes use of, is described as follows.

Definition 2. (Triad condition) Suppose assumptions **A1** - **A3** hold. For a triple of measured variables (X_i, X_j, X_k) generated by (1). X_j and X_k are Triad conditional on X_i (or given X_i), when the residual $E_{X_k, X_j | X_i} = X_k - \frac{\text{Cov}(X_i, X_k)}{\text{Cov}(X_i, X_j)} \cdot X_j$ is independent of X_i , that is, $E_{X_j, X_k | X_i} \perp\!\!\!\perp X_i$. If the Triad condition is satisfied, we denote it by $\text{Triad}(X_j, X_k | X_i)$.

It is easy to establish the property that the Triad condition is symmetric, that is, $\text{Triad}(X_j, X_k | X_i)$ if and only if $\text{Triad}(X_k, X_j | X_i)$.

The three possible causal graphs given in Figures 5 (a)-(c) over three measured variables (X_i, X_j, X_k) correspond to the PAG in Figure 5 (d) that is produced by stage I. None of the three undirected edges can be reoriented by stage II. Based on the Triad condition, We detect whether three variables share a latent confounder via the following Theorem 4.

Theorem 4. Suppose that the data over variables \mathbf{X} was generated according to Equation 1 and assumptions **A1** – **A4** hold. Let \mathcal{G}_2 denote the output of stage II of FRITL. For three observed variables (X_i, X_j, X_k) with an undetermined edge between each pair of them in \mathcal{G}_2 , if and only if three Triad conditions hold among (X_i, X_j, X_k) , then (X_i, X_j, X_k) are directly influenced by a same latent confounder, and each pair of observed variables are not directly connected.

Proof. Suppose that the data over variables \mathbf{X} was generated by Equation 1. Without loss of generality, we assume three variables in \mathbf{X} , X_i , X_j and X_k , are standardized (they have a zero mean and a unit variance) and have causal relations in between, in addition to the influences of latent confounders. Note that if a coefficient is zero, then the corresponding edge vanishes. Then we have

$$\begin{aligned} X_i &= \Lambda_i \mathbf{L} + E_i, \\ X_j &= b_{j,i} X_i + \Lambda_j \mathbf{L} + E_j, \\ X_k &= b_{k,i} X_i + b_{k,j} X_j + \Lambda_k \mathbf{L} + E_k. \end{aligned} \tag{11}$$

Three kinds of Triad conditions might hold among three variables: $Triad(X_j, X_k | X_i)$, $Triad(X_i, X_k | X_j)$ and $Triad(X_i, X_j | X_k)$. So we consider three cases conditioning on different variables as follows.

1. Considering a Triad condition conditioning on X_i , we can obtain the following reference variable

$$\begin{aligned} E_{X_k, X_j | X_i} &= X_k - \frac{\text{Cov}(X_i, X_k)}{\text{Cov}(X_i, X_j)} \cdot X_j \\ &= (b_{k,i} X_i + b_{k,j} X_j + \Lambda_k \mathbf{L} + E_k) - \frac{b_{k,i} + \Lambda_i \Lambda_k^T}{b_{j,i} + \Lambda_i \Lambda_j^T} \cdot (b_{j,i} X_i + \Lambda_j \mathbf{L} + E_j) \\ &= \frac{b_{j,i} \Lambda_k - b_{k,i} \Lambda_j}{b_{j,i} + \Lambda_i \Lambda_j^T} \cdot \mathbf{L} + \frac{(b_{k,i} \Lambda_i \Lambda_j^T - b_{j,i} \Lambda_i \Lambda_k^T)}{b_{j,i} + \Lambda_i \Lambda_j^T} \cdot X_i - \frac{b_{k,i} + \Lambda_i \Lambda_k^T}{b_{j,i} + \Lambda_i \Lambda_j^T} \cdot E_j + E_k \\ &= \frac{\Lambda_i \Lambda_i^T \cdot (b_{k,i} \Lambda_j - b_{j,i} \Lambda_k)}{b_{j,i} + \Lambda_i \Lambda_j^T} \cdot \mathbf{L} + \frac{(b_{k,i} \Lambda_i \Lambda_j^T - b_{j,i} \Lambda_i \Lambda_k^T)}{b_{j,i} + \Lambda_i \Lambda_j^T} \cdot E_i \\ &\quad - \frac{\Lambda_i \Lambda_k^T + b_{k,i}}{b_{j,i} + \Lambda_i \Lambda_j^T} \cdot E_j + E_k, \end{aligned}$$

which is a linear mixture of independent variables, namely, \mathbf{L} , E_i , E_j , and E_k . As we know, X_i is a mixture of independent variables \mathbf{L} and E_i . If the parameters in this model are not zero, it is dependent on X_i because of Theorem 2. Next, if it satisfies $Triad(X_j, X_k | X_i)$, i.e., $E_{X_k, X_j | X_i}$ is independent of X_i . According to Theorem 2, at most one of the coefficients of their common parameters, \mathbf{L} and E_i should be zero. Therefore, $\frac{\Lambda_i \Lambda_i^T \cdot (b_{k,i} \Lambda_j - b_{j,i} \Lambda_k)}{b_{j,i} + \Lambda_i \Lambda_j^T}$ and $b_{k,i} \Lambda_i \Lambda_j^T - b_{j,i} \Lambda_i \Lambda_k^T$ should be equal to zero, i.e., $b_{j,i} = b_{k,i} = 0$, because Λ_i , Λ_j and Λ_k are nonzero. Then, $E_{X_k, X_j | X_i}$ becomes a linear mixture of E_j , and E_k and is independent of X_i . Thus, there are no edges between X_i and X_j , and between X_k and X_i .

2. Consider a Triad condition conditioning on X_j , we can obtain the following reference variable

$$\begin{aligned}
E_{X_k, X_i | X_j} &= X_k - \frac{\text{Cov}(X_k, X_j)}{\text{Cov}(X_i, X_j)} \cdot X_i \\
&= (b_{k,i} X_i + b_{k,j} X_j + \Lambda_k \mathbf{L} + E_k) - (b_{k,i} + \frac{\Lambda_k \cdot (\Lambda_j^T + b_{j,i} \Lambda_i^T) + b_{k,j}}{b_{j,i} + \Lambda_i \Lambda_j^T}) \cdot X_i \\
&= (\Lambda_k \cdot \mathbf{L} + b_{k,j} \cdot (b_{j,i} X_i + \Lambda_j \mathbf{L} + E_j) + E_k) - \frac{\Lambda_k \cdot (\Lambda_j + b_{j,i} \Lambda_i) + b_{k,j}}{b_{j,i} + \Lambda_i \Lambda_j^T} \cdot X_i \\
&= (b_{k,j} b_{j,i} \Lambda_i + b_{k,j} \Lambda_j + \Lambda_k - \frac{(\Lambda_k \Lambda_j^T + b_{j,i} \Lambda_k \Lambda_i^T + b_{k,j}) \Lambda_i}{b_{j,i} + \Lambda_i \Lambda_j^T}) \cdot \mathbf{L} \\
&\quad - (b_{k,j} b_{j,i} - \frac{\Lambda_j \Lambda_k^T + b_{j,i} \Lambda_i \Lambda_k^T + b_{k,j}}{b_{j,i} + \Lambda_i \Lambda_j^T}) \cdot E_i + b_{k,j} \cdot E_j + E_k,
\end{aligned}$$

which is a linear mixture of four independent variables, namely, \mathbf{L} , E_i , E_j , and E_k . We can see that

$$X_j = b_{j,i} X_i + \Lambda_j \mathbf{L} + E_j = (b_{j,i} \Lambda_i + \Lambda_j) \cdot \mathbf{L} + b_{j,i} \cdot E_i + E_j, \quad (12)$$

which is a mixture of three independent variables \mathbf{L} , E_i and E_j . If all parameters in this model are non-zero, $E_{X_k, X_i | X_j}$ is dependent of X_j because of the Theorem 2.

If all three variables are directly influenced by the same latent confounder, satisfies $\text{Triad}(X_i, X_k | X_j)$, i.e., $E_{X_k, X_i | X_j}$ is independent of X_j . According to Theorem 2, at most one of the coefficients on their common parameters, \mathbf{L} , E_i and E_j , should be zero. Therefore, $b_{k,j}$ would be zero, and then we can see that $b_{j,i}$ would be zero, too. Then, $E_{X_k, X_i | X_j}$ becomes a linear mixture of E_i and E_k , and is independent of X_j . This also shows that the graph in which there is at most one directed edge between two measured variables and one latent confounder influences them at the same time are distinguishable by the Triad condition.

3. Consider a Triad conditioning on X_k , similar with the two cases above, we can know that if there is only one edge between X_i and X_j , i.e., $b_{k,j} = b_{k,i} = 0$, then the graph implies Triad condition $\text{Triad}(X_i, X_j | X_k)$.

In conclusion, if there is not a directed edge between any pair of measured variables, that is, $b_{j,i} = b_{k,j} = b_{k,i} = 0$, then the corresponding causal graph implies three Triad conditions, which are $\text{Triad}(X_j, X_k | X_i)$, $\text{Triad}(X_i, X_k | X_j)$, $\text{Triad}(X_i, X_j | X_k)$. According to assumption **A3**, $b_{j,i} = 0$ means that there is no direct edge between observed variables X_i and X_j . If at least two causal strengths in $\{b_{j,i}, b_{k,j}, b_{k,i}\}$ are zero, then the causal structure over (X_i, X_j, X_k) satisfied one of the graph given in Figure 6. For three variables that are mutually adjacent with undetermined edges in the sub-graph of \mathcal{G}_2 , if there exist one observed variable that is not adjacent to other two observed variables, then stage III

of FRITL is able to identify these observed variables are influenced by the same latent confounder. \square

Theorem 4 provides a criterion for detecting the latent confounders that directly influence three (or more) measured variables. Therefore, let \mathcal{G}_2 be the graph produced by stage II. We test Triad conditions on every triple of variables with undetermined edges among them in \mathcal{G}_2 , and determine whether these three variables are influenced by a same latent confounder according to Theorem 4. For example, in Figure 3(c), the triple X_5, X_7, X_8 satisfies three Triad conditions. We remove the edges among X_5, X_7 and X_8 and record that they are influenced by the same latent confounder. The output of stage III is given as Figure 3(d). After this stage, we can group some variables that are directly influenced by the same latent confounders, and eliminate more undetermined edges.

From the proof of Theorem 4, if only one Triad condition is satisfied among three variables with undetermined edges in between, then the undetermined sub-graph might be one of the four cases given in Figure 6. With the help of Triad conditions, we can further apply overcomplete ICA to select the best model if needed.

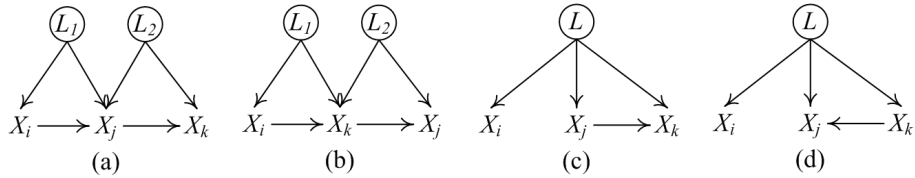


Figure 6: Four causal structures corresponding to the PAG given in Figure 5 and satisfying the Triad condition $Triad(X_j, X_k | X_i)$.

If we cannot find any Triad conditions among the considered triple of variables, then the original causal graph belongs to one of the following cases:

- There are two or more than two directed edges between the three measured variables in the original causal graph, in which these variables are directly influenced by the same latent confounder;
- Each pair of the three measured variables is directly influenced by a latent confounder, as in Figure 5 (c).

4.4 Stage IV: Estimating Remaining Undetermined Local Structures Using Overcomplete ICA

In the general case, some undetermined edges not identified by the previous stages might remain. For example, in Figure 3(d), the edge between X_4 and X_7 cannot be determined by the preceding stages. We now apply overcomplete ICA locally to identify the local

undetermined causal structures, that is, using overcomplete ICA only on the data of X_4 and X_7 after regressing their known parents out in order to remove the common causal effects.

According to Hoyer et al. (2008), two latent variable LiNGAM models are observationally equivalent if and only if the distribution P of the observed data is identical for these two models. A latent variable LiNGAM model, where each latent variable is a root node (i.e., has no parents) and has at least two children (direct descendants), is a canonical model. Under assumption **A3**, we note that \mathbf{A} in Equation 2 can be estimated up to the permutation and scaling of the columns, as given in the following lemma.

Lemma 5. *If assumptions **A1-A4** are true, and \mathbf{X} is generated according to (2), \mathbf{A} is identifiable up to permutation and scaling of columns. All the causal structure is identified up to observationally equivalent canonical models.*

Proof. This lemma is implied by Theorem 10.3.1 in Kagan et al. (1973) or Theorem 1 in Eriksson and Koivunen (2004). It is also proven in Hoyer et al. (2008). \square

Let \mathcal{G}_3 be the graph obtained by stage III with undetermined edges. If \mathcal{G}_3 has many variables with undetermined edges in between, applying overcomplete ICA on all of them together has a very high procedural complexity with limited estimation accuracy. Stage II determines all unconfounded edges, and the variables with undetermined edges in between are directly influenced by latent confounders. We notice that if several measured variables are directly influenced by the same confounder, then a clique forms in the output of Stage II, with an underdetermined edge between each pair of them. Stage III, with output \mathcal{G}_3 , already identifies a special case where multiple variables share the same confounder by checking for the Triad condition. Taking this further, we must figure out whether the variables are directly influenced by the same latent confounders. To do so, we consider the subsets of the variables forming a maximal clique involving only undetermined edges and then apply overcomplete ICA to estimate their causal structure. We understand that it is not necessary for the variables in the same maximal clique to be directly influenced by the same confounder, as seen in the structure given in Figure 5 (c).

Specifically, we consider only the undetermined edges in \mathcal{G}_3 , and separate relevant variables into different (possibly overlapping) maximal cliques with all edges undetermined in each. For variables in the same maximal clique, we estimate the causal structure together with the influences from confounders. For each maximal clique, it is possible for all variables in the maximal clique to be directly influenced by a few or even one latent confounder. As a consequence, we apply overcomplete ICA on each complete maximal clique, and the number of latent confounders can be estimated by model selection, if needed.

Considering the example in Figure 7, we apply the first three stages of our method over the data generated by Figure 7(a) to obtain Figure 7(b). We then apply overcomplete ICA on the variables in the two maximal cliques (with undetermined edges), given in Figure 7(c), separately, recovering the two local causal structures.

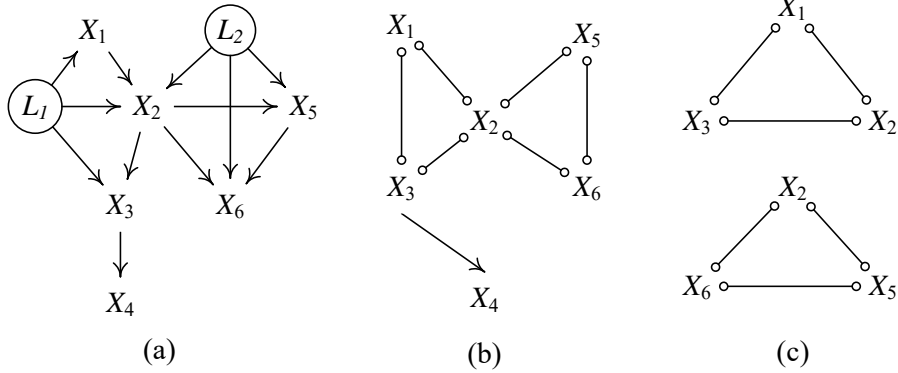


Figure 7: An example for stage IV: (a) true causal graph; (b) a PAG corresponding to (a), produced by stage III; and (c) two undetermined maximal cliques separated from (b).

5. Discussion

In this section, we show how the first three stages of our method make overcomplete ICA more accurate and efficient.

Consider a true causal structure among one of the graphs shown in Figure 6 that satisfies $Triad(X_j, X_k | X_i)$. In practice, exclusively using overcomplete ICA to discover the causal structure without applying stages I–III first, the algorithm needs to iterate all possible causal structures with permutation and scaling of columns of \mathbf{A} to find the best model. Moreover, because the number of latent confounders N_L is unknown, we need to test all cases based on all possible numbers of N_L . As the number of measured variables increases, more cases need to be computed, with a greater probability of falling into a local maximum. In contrast, stages I and II of our method return only the causal graph given in 5 (d), but the use of Triad condition in Stage III determines that the causal structures must be among the graphs given in Figure 6. We need to perform overcomplete ICA only on these four possible causal structures, returning only the best one rather than estimating the causal structures in a large space with different numbers of latent confounders and possible causal graphs. In this case, the use of Triad condition greatly reduces the search space and identifies possible sub-structure informed by the previous result, as shown in Figure 5 (a).

Hence, we can determine the unconfounded structures by stage II, and further determine some sub-structures over three (or more) observed variables with latent confounders by stage III. These stages not only make the FCI result more informative, but can reduce the search space when using overcomplete ICA if needed. Further, our method is less prone to local optima and more efficient.

6. Experiments

In this section, we conduct simulation experiments and apply our method to real-world data to evaluate our method’s performance.

6.1 Synthetic data

We performed simulations as follows. We randomly generated causal structures over measured variables and latent confounders with different average *indegree* = 0.5, 1, 1.5, 2, 2.5, 3, 3.5, which are the ratios of the number of indegree edges to the number of measured variables. Each causal structure had 10 measured variables. In each generated graph, we randomly designed different ratios of latent confounders on the number of measured variables, $p = 0.1, 0.2, 0.3, 0.4, 0.5$. Data for these variables were not given to the search procedure. The maximum number of children for each latent confounder was 3. Based on each causal structure, we generated the data according to LvLiNGAM, with the causal strength between different variables randomly chosen in the range of $(-1, -0.2] \cup [0.2, 1)$ and the noise term for each variable randomly chosen from the uniform distribution on the interval $[-0.5, 0.5]$. In addition, our generated data consisted of 1000 samples in each set. For each setting, we repeated the algorithm 50 times, each time randomly generating a causal graph and coefficient, and then sampling a data set.

In these experiments, we used the FCI Java implementation from the Tetrad¹ for stage I of our method. Pseudo-code for FCI is described in Spirtes et al. Spirtes et al. (2001). For the regression and independence test, we used least squares regression to perform linear regressions and the kernel-based conditional independence (KCI) test Zhang et al. (2011) to conduct (conditional) independence tests between variables. Here we used 0.05 as the significance level for the independence test. In these experiments, we evaluated the performance of our method in terms of arrowheads among measured variables of recovered causal graphs and pairs of measure variables that were detected to be directly influenced by latent confounders, by computing precision, recall, and F1 score. Precision is the percentage of correct causal edges between measured variables among all causal edges returned by the algorithm. Recall is the percentage of correct causal edges that are found by the search among true causal edges between measured variables. The F1 score is defined as

$$F1score = \frac{2 \times precision \times recall}{precision + recall}. \tag{13}$$

To show the performance of different stages of our method, we also applied FCI (stage I), FRI (the combination of stages I and stage II), FRIT (the combination of first three stages), and FRITL (all stages) in the generated data sets. To show the performance of our framework, we used PairwiseLvLiNGAM Entner and Hoyer (2010) as the second phase of the framework, calling the new method FCI-pw. Besides, we utilized ParceLiNGAM Tashiro

1. www.phil.cmu.edu/tetrad/

et al. (2014) that can be against the latent confounders as another compared method, and DirectLiNGAM Shimizu et al. (2011) that assumes causal sufficiency to evaluate whether the performance of algorithm considering latent confounders is better.

Figure 8 gives the performance of our methods for the arrowheads. In this figure, the y-axis is precision, recall, or F1 score; a higher value means higher accuracy.

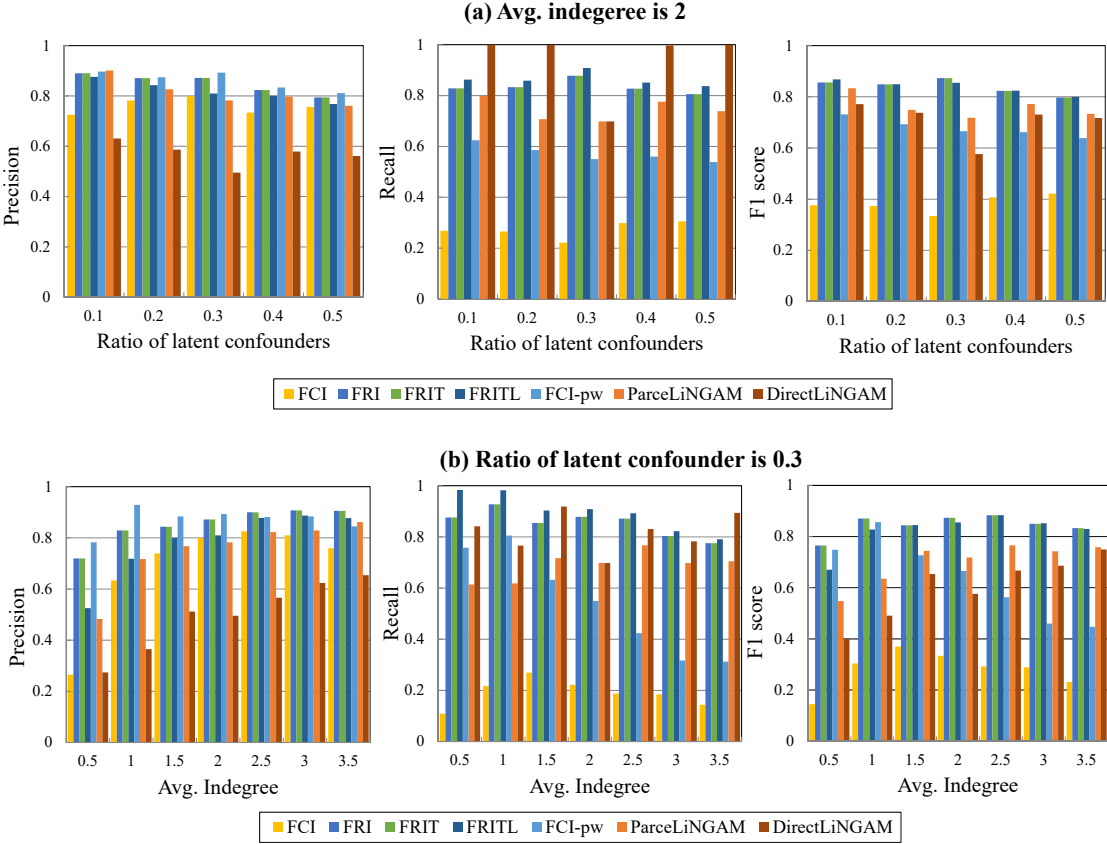


Figure 8: The evaluation of arrowheads among measured variables of recovered causal graphs.

Sensitivity of different settings in arrowheads among measured variables. From Figure 8, we can see that the performance of FRI and FRIT are the same. This is because the stage III of our algorithm does not refine the causal directions between measured variables. The precision of FCI is mostly higher than 0.7, while the recall is smaller than 0.4, indicating that causal directions found by FCI are correct but with many undetermined causal edges remaining. Our method works better than FCI in both precision and recall,

indicating the presence of more information. In all cases, FRI’s precision was higher than that of FRITL while FRI’s recall was lower than that of FRITL. This indicates that stage IV of our algorithm - with overcomplete ICA technique, correctly estimate some undetermined edges but introduce some redundant edges, which shows this technique is not reliable. The results of FRI and FCI-pw show nearly identical precision when the causal graph has a sparseness of 2, with FRI having higher recall. This shows that the causal directions found by pairwiseLiNGAM are nearly correct, but most confounded edges, both latent and observed, could not be determined. Our method successfully finds confounded edges or indirect latent confounded edges by comparison. Compared with ParceLiNGAM, our method performs better, even when the ratio of the latent confounder is 5, further showing the effectiveness of our algorithm. Our method’s higher F1 score compared to DirectLiNGAM reflects the importance of taking latent confounders into account. Figure 8 (a) shows our method to be mostly stable in the precision of arrowheads, which means stages II and III of our method are good for determining the causal direction of the PAG produced by FCI. In Figure 8 (b) shows that the recall of our method decreases as the graph density increases, with precision increasing. This means stages II and III of our method does not determine many causal edges between measured variables influenced by latent confounders. In summary, these results demonstrate the correctness and effectiveness of our method, with an ability to use a number of stages appropriate to the data if needed.

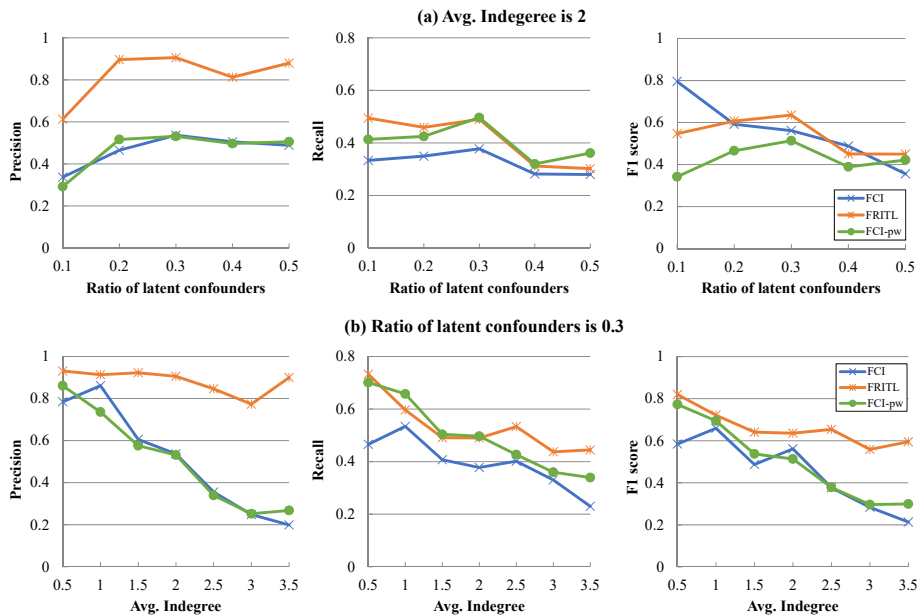


Figure 9: The evaluation of the pairs of measure variables detected to be directly influenced by latent confounders.

Sensitivity of different settings in the pairs of measure variables that are detected to be directly influenced by latent confounders. Our method also determines latent confounder influences which measured variables. Because ParceLiNGAM and DirectLiNGAM cannot do so, we only evaluate the performance of our method on the pairs of measure variables that are detected to be directly influenced by latent confounders, and compare them with the results produced by FCI and FCI-pw. As a reminder, FCI-pw only determines the unconfounded pairs of measured variables, so we treat the undetermined pair as directly influenced by the same latent confounder. As before, we evaluated the results according to the precision, recall, and F1 score. The results are given in Figure 9. Figure 9(a) shows that when the ratio of latent confounders is larger than 0.2, the precision of our method is larger than 0.8 whereas those that of FCI and FCI-pw are only around 0.6. The recall of FCI-pw is higher than that of our method in most cases. This indicates FCI-pw does not find pairs not influenced by latent confounders, and the ones that our algorithm found are correct. Figure 9(b) shows that when the number of latent confounders increases, the precision of method’s recovery of the causal relationships between observed and latent variables lightly increases slightly whereas that of the results learned by FCI and FCI-pw decreases, which illustrates that our method finds more true latent confounders and recovers more causal relations between latent confounders and measured variables even in a dense graph. Although the recall of our algorithm is lower than that of FCI-pw when the average indegree of the causal graph is 1 and 1.5, the F_1 score of our algorithm is higher. All of these figures show that our methods correctly recover most measured variables that are directly influenced by latent confounders.

6.2 FMRI Task Data

To test the performance of our method in a real problem, we applied our method to real functional magnetic resonance imaging (fMRI) task data previously published in Ramsey et al. (2010). These data sets consist of 9 subjects that are judged whether a pair of visual stimuli rhymed or not. Data was acquired with a 3T scanner, with $TR = 2$ seconds, so the sample size for each subject is 160 Sanchez-Romero et al. (2019). Raw data is available at the OpenfMRI Project²; and the preprocessed data used here is available³. We use the preprocessed data in this experiment.

In these data sets, each subject has 9 variables, which are one input variable (Input) and eight regions of interest (ROIs). The Input variable is built by convolving the rhyming task boxcar model with a canonical hemodynamic response function. The eight ROIs are left and right occipital cortex (LOCC, ROCC); left and right anterior cingulate cortex (LACC, RACC); left and right inferior frontal gyrus (LIFG, RIFG); left and right inferior parietal (LIPL, RIPL).

2. <https://openfmri.org/dataset/ds000003/>

3. <https://github.com/cabal-cmu/Feedback-Discovery>

We applied our method and FCI on the concatenated data set for the Input variable and the eight regions of interest. This data set is combined by 1 repetition of 9 standardized individual data sets. Accordingly the sample size of this data set is 1440. The threshold for the independence tests in this experiment is 0.01. Figure 10 gives the output graphs produced by FRITL and FCI, respectively.

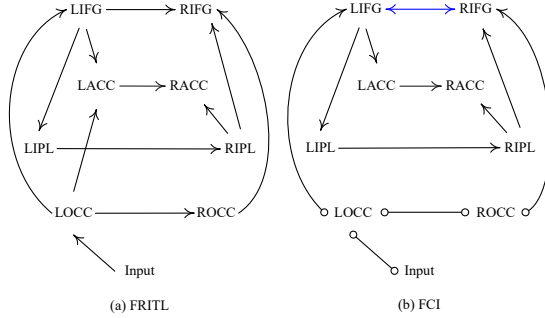


Figure 10: The output graphs produced by different methods on concatenated data set for eight bilateral regions of interest and one Input variable. The blue line denotes that there is a latent confounder for the adjacent measured variables.

Compared fMRI task data with synthetic data, a shared common view is that stimulus input should go to the left occipital, feed upwards, and feed from left to right. Thus, the Input variables should be the exogenous variable in the true graph. From Figure 10, we can see that FRITL correctly outputs the edges from the Input variable to the region of interest, while FCI correctly outputs the adjacency on these edges but did not orient them. Figure 10(b) shows that there are four undetermined edges in the output of FCI, which are refined by our method (Figure 10(a)). It proves that the output of FCI is less informative than that of our method. From the results, we also show that the ROIs in the left hemisphere always be the causes of that in the right hemisphere, which is consistent with the common view.

6.3 Sachs Data

We also applied FRITL, FCI-pw, FCI, ParceLiNGAM, and DirectLiNGAM to Sachs data Sachs et al. (2005). Sachs data records many cellular protein concentrations in single cells. This data contains 9 files with varying interventions. In this experiment, we use these intervention knowledges so that the data contains 11 measured variables and 7466 samples. Figure 11 shows the results of FRITL, FCI, ParceLiNGAM, and DirectLiNGAM. We also visualize the ground-truth given in Figure 11 for evaluation. The results show that FCI-pw did not refine any edges from the FCI result, while FRITL reorientated two edges and located the latent confounders. ParceLiNGAM failed to find the causal order of 9 variables

except for *Mek* and *Raf*, meaning it could not determine the causal relationships among most of the variables. it performs pruning, DirectLiNGAM still outputs many redundant causal edges. This is because the presence of latent confounder for two observed variables introduced false causal relationships among these observed variables. This demonstrates the importance of considering the existence of latent confounders. Comparing FRITL output and the ground truth, the causal graph estimated by our method does not contain the *Mek* \rightarrow *Erk* edge, which is well-established.

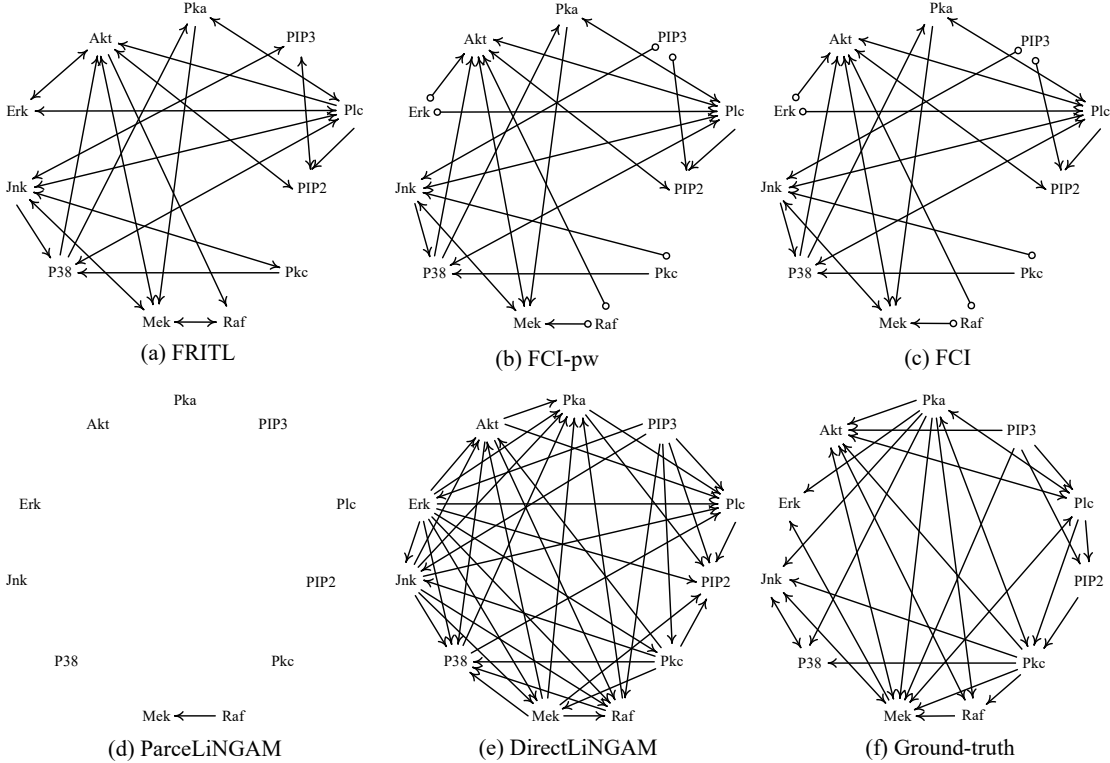


Figure 11: (a) - (e) The results of different methods applied in Sachs data. (f) The ground truth.

7. Conclusions

In this paper, we provide a hybrid method to reconstruct a causal graph of observed variables and latent confounders. In the proposed framework, we use FCI to decompose the global structure and use the independence noise condition, Triad condition, and overcomplete ICA to infer remaining local structures. The simulated experiments results show

that FRITL is asymptotically correct and is more informative than FCI. In application to real functional magnetic resonance data and Sachs data, FRITL yields results in good agreement with neuropsychological opinion and precise agreement a causal relation known from the experimental design. In the future, we would like to generalize this framework to nonlinear cases.

Acknowledgments

Wei Chen would like to thank the CABAL group at Carnegie Mellon University for insightful discussion and suggestions. This research was supported in part by National Natural Science Foundation of China (61876043), Science and Technology Planning Project of Guangzhou (201902010058). Wei Chen would like to gratefully acknowledge the financial support from China Scholarship Council (CSC) and the Outstanding Young Scientific Research Talents International Cultivation Project Fund of Department of Education of Guangdong Province.

References

- Ruichu Cai, Zhenjie Zhang, Zhifeng Hao, and Marianne Winslett. Understanding social causalities behind human action sequences. *IEEE transactions on neural networks and learning systems*, 28(8):1801–1813, 2016.
- Ruichu Cai, Xie Feng, Clark Glymour, Hao Zhifeng, and Kun Zhang. Triad constraints for learning causal structure of latent variables. In *Advances in Neural Information Processing Systems*, 2019.
- Tom Claassen, Joris M Mooij, and Tom Heskes. Learning sparse causal models is not np-hard. In *Uncertainty in Artificial Intelligence*, page 172. Citeseer, 2013.
- Diego Colombo and Marloes H Maathuis. Order-independent constraint-based causal structure learning. *The Journal of Machine Learning Research*, 15(1):3741–3782, 2014.
- Diego Colombo, Marloes H Maathuis, Markus Kalisch, and Thomas S Richardson. Learning high-dimensional directed acyclic graphs with latent and selection variables. *The Annals of Statistics*, pages 294–321, 2012.
- George Darmon. Analyse générale des liaisons stochastiques: etude particulière de l’analyse factorielle linéaire. *Revue de l’Institut international de statistique*, pages 2–8, 1953.
- Doris Entner and Patrik O Hoyer. Discovering unconfounded causal relationships using linear non-gaussian models. In *JSAI International Symposium on Artificial Intelligence*, pages 181–195. Springer, 2010.

- Jan Eriksson and Visa Koivunen. Identifiability, separability, and uniqueness of linear ica models. *IEEE signal processing letters*, 11(7):601–604, 2004.
- Patrik O Hoyer, Shohei Shimizu, Antti J Kerminen, and Markus Palviainen. Estimation of causal effects using linear non-gaussian causal models with hidden variables. *International Journal of Approximate Reasoning*, 49(2):362–378, 2008.
- Abram Kagan, IUrii Vladimirovich Linnik, and Calyampudi Radhakrishna Rao. *Characterization problems in mathematical statistics*. Wiley series in probability and mathematical statistics. Wiley, 1973. ISBN 9780471454212. URL <https://books.google.com/books?id=kQqoAAAAIAAJ>.
- Michael S Lewicki and Terrence J Sejnowski. Learning overcomplete representations. *Neural computation*, 12(2):337–365, 2000.
- Juan Miguel Ogarrio, Peter Spirtes, and Joe Ramsey. A hybrid causal search algorithm for latent variable models. In *Conference on Probabilistic Graphical Models*, pages 368–379, 2016.
- Judea Pearl. *Probabilistic Reasoning in Intelligent Systems: Networks of Plausible Inference*. Morgan Kaufmann, 1988.
- Joseph Ramsey, Peter Spirtes, and Jiji Zhang. Adjacency-faithfulness and conservative causal inference. In *Proceedings of the Twenty-Second Conference on Uncertainty in Artificial Intelligence*, pages 401–408. AUAI Press, 2006.
- Joseph D Ramsey, Stephen José Hanson, Catherine Hanson, Yaroslav O Halchenko, Russell A Poldrack, and Clark Glymour. Six problems for causal inference from fmri. *neuroimage*, 49(2):1545–1558, 2010.
- Karen Sachs, Omar Perez, Dana Pe’er, Douglas A Lauffenburger, and Garry P Nolan. Causal protein-signaling networks derived from multiparameter single-cell data. *Science*, 308(5721):523–529, 2005.
- Ruben Sanchez-Romero, Joseph D Ramsey, Kun Zhang, Madelyn RK Glymour, Biwei Huang, and Clark Glymour. Estimating feedforward and feedback effective connections from fmri time series: Assessments of statistical methods. *Network Neuroscience*, 3(2):274–306, 2019.
- Shohei Shimizu, Takanori Inazumi, Yasuhiro Sogawa, Aapo Hyvärinen, Yoshinobu Kawahara, Takashi Washio, Patrik O Hoyer, and Kenneth Bollen. Directlingam: A direct method for learning a linear non-gaussian structural equation model. *Journal of Machine Learning Research*, 12(Apr):1225–1248, 2011.
- VP Skitovitch. On a property of the normal distribution. *DAN SSSR*, 89:217–219, 1953.

Peter Spirtes, Clark Glymour, and Richard Scheines. Causation, prediction, and search, second edition. *The MIT Press*, 2001.

Tatsuya Tashiro, Shohei Shimizu, Aapo Hyvärinen, and Takashi Washio. Parcelingam: a causal ordering method robust against latent confounders. *Neural computation*, 26(1): 57–83, 2014.

Jiji Zhang. On the completeness of orientation rules for causal discovery in the presence of latent confounders and selection bias. *Artificial Intelligence*, 172(16-17):1873–1896, 2008.

Kun Zhang, Jonas Peters, Dominik Janzing, and Bernhard Schölkopf. Kernel-based conditional independence test and application in causal discovery. In *Proceedings of the Twenty-Seventh Conference on Uncertainty in Artificial Intelligence*, UAI'11, pages 804–813, Arlington, Virginia, United States, 2011. AUAI Press. ISBN 978-0-9749039-7-2. URL <http://dl.acm.org/citation.cfm?id=3020548.3020641>.